



**HAL**  
open science

## **ROMANS' ESTABLISHED SKILLS: MORTARS FROM D46b MAUSOLEUM, PORTA MEDIANA NECROPOLIS, CUMA (NAPLES)**

Claudia Di Benedetto, Sossio Fabio Graziano, Vincenza Guarino, Concetta Rispoli,  
Priscilla Munzi, Vincenzo Morra, Piergiulio Cappelletti

### ► **To cite this version:**

Claudia Di Benedetto, Sossio Fabio Graziano, Vincenza Guarino, Concetta Rispoli, Priscilla Munzi, et al.. ROMANS' ESTABLISHED SKILLS: MORTARS FROM D46b MAUSOLEUM, PORTA MEDIANA NECROPOLIS, CUMA (NAPLES). *Mediterranean Archaeology and Archaeometry*, 2018, 18, pp.131 - 146. <10.5281/zenodo.1285895>. <hal-01861835>

**HAL Id: hal-01861835**

**<https://hal.science/hal-01861835v1>**

Submitted on 18 Nov 2018

**HAL** is a multi-disciplinary open access archive for the deposit and dissemination of scientific research documents, whether they are published or not. The documents may come from teaching and research institutions in France or abroad, or from public or private research centers.

L'archive ouverte pluridisciplinaire **HAL**, est destinée au dépôt et à la diffusion de documents scientifiques de niveau recherche, publiés ou non, émanant des établissements d'enseignement et de recherche français ou étrangers, des laboratoires publics ou privés.



HAL Authorization



DOI: 10.5281/zenodo.1285895

## **ROMANS' ESTABLISHED SKILLS: MORTARS FROM D46b MAUSOLEUM, *PORTA MEDIANA NECROPOLIS*, CUMA (NAPLES)**

**Claudia Di Benedetto<sup>\*1</sup>, Sossio Fabio Graziano<sup>1</sup>, Vincenza Guarino<sup>1</sup>, Concetta Rispoli<sup>1</sup>,  
Priscilla Munzi<sup>2</sup>, Vincenzo Morra<sup>1</sup>, Piergiulio Cappelletti<sup>1</sup>**

<sup>1</sup>*DiSTAR - Dipartimento di Scienze della Terra, dell'Ambiente e delle Risorse - Università di Napoli  
Federico II, Via Cintia, 26 - Napoli.*

<sup>2</sup>*Centre Jean Bérard, USR 3133 CNRS - École française de Rome, Via Francesco Crispi, 86 - Napoli*

Received: 17/12/2017

Accepted: 20/02/2018

*\*Corresponding author: Claudia Di Benedetto (claudia.dibenedetto@unina.it)*

### **ABSTRACT**

Roman mortars from a mausoleum (named D46b) belonging to the archaeological site of *Porta Mediana necropolis*, in Cuma (Naples, Southern Italy) have been studied by means of petrographic, mineralogical and micro-chemical analyses. The aim of this research is to fill the knowledge gap regarding mortar-based materials used in Roman age within this wide archaeological site.

Two typologies of mortars (bedding and coating) were collected from mausoleum's masonry. They were lime-based with addition of pozzolanic materials, according to Vitruvius' recipe.

Raw materials, such as volcanic sand and limestones, mainly from local sources, were preferentially used as aggregate, both for great availability and good properties.

As regard production techniques, the multi-layer feature of the coating mortars, once again shows the great knowledge of the building art. Each layer is the result of a precise choice, as shown by the differences both in texture and petrographic features.

Data from detailed mortars characterization have infer the outstanding skill of Roman craftsmen, as already proved by extraordinary durability of buildings.

The research was very useful not only to increase the knowledge of this ancient culture but also to planning conservative actions, that, through mortar reproduction or the research of suitable materials, can promote the safeguard of this invaluable heritage.

---

**KEYWORDS:** roman mortars, bedding, coating, raw materials, volcanic aggregate, technology

---

## 1. INTRODUCTION

Mortars represent one of the most important artificial building materials, used since Roman times (Collepari, 2003; Elsen, 2006; Pecchioni et al., 2008, 2009). They are composite materials, characterized by natural aggregates added in lime binder, often related both to the place and the historical time in which they are made (Pecchioni et al. 2008; Collepari et al., 2003). Roman mortars were used with different function: plasters (renders), on internal and external walls, supporting substrates for frescoes bedding mortars of masonry supporting materials for pavements or mosaics and watertight lining materials in cisterns, wells, aqueducts etc.. (Moropolou et al., 2000).

Outstanding examples of well-preserved Roman mortars can be found in Campania region, with its considerable number of archaeological sites, where interests of researchers were focused.

Several studies mainly involved Vesuvian archaeological sites, such as *Pompei* (Bonazzi et al., 2007; Castriota et al., 2008; De Luca et al., 2015; Miriello et al., 2010; Piovesan et al., 2013), *Ercolano* (Leone et al., 2016; De Vita et al., 2010), and *Stabia* (Izzo et al., 2016). Within Phlegraean Fields area, instead, investigations have been carried out mainly on the nowadays underwater heritage of Baia (Aloise et al., 2013; La Russa et al., 2015; Ricci et al., 2009), while very few on emerged ones, as *Piscina Mirabilis* and *Terme di Baia* sites (Rispoli et al., 2015, 2016), although they represent an invaluable archaeological heritage. Relevant archaeometric studies on mortars have been quoted in other cases (Liritzis et al., 2015; Salama et al., 2017).

One of the most important archaeological site of Phlegraean Fields is the area of Cuma, which represents the oldest Greek colony of the Occident. In this wide archaeological area, a Necropolis, named *Porta Mediana*, was revealed by the *Centre Jean Berard* archaeologists, between 2001 and present. The *Porta Mediana* necropolis consists of about 70 funerary monuments, ranging from 2nd BC and 6th century AD, developed in different building phases (Brun & Munzi, 2008; Brun et al., 2017). This site, in which geology and archeology are deeply related, was involved in a systematic study of natural and artificial geomaterials, carried out by strictly collaboration between DiSTAR and *Centre Jean Bérard*, within the

*SINAPSIS* Project (PON - *Sistema Nazionale Protezione Siti Sensibili*).

Aim of this research is provide, by means of mineralogical and petrographic investigations, a full characterization of mortars from masonry boundaries of specific area, which includes a funerary monument, named D46b (1<sup>st</sup> century BC) and following commercial buildings (2<sup>nd</sup> - 3<sup>rd</sup> century AD). The main goal is fill the gap of knowledge about raw materials, their provenance and availability in the studied area. To this purpose the choice as fell on this area because it represents an important part of a complex stratigraphy sequence identified in this sector of *Necropolis*. Due to its strategic position along the oldest route of the *Necropolis* (dating back from archaic era; Brun et al., 2013), this funerary monument can provide useful preliminary information to understand the chronological building evolution of the *Porta Mediana* site (Brun et al., 2013).

## 2. GEOLOGICAL SETTING

The archaeological site of *Cuma* is located in the north-western sector of Phlegraean Fields volcanic district (*Campania* region, Southern Italy; Morra et al., 2010; Fedele et al., 2011; Fig. 1), that, along with *Somma-Vesuvius*, represent the two main still active, quaternary volcanoes in the Mediterranean area.

The volcanic activity, mainly explosive, deeply affected the morphology of the area, also providing geomaterials suitable for building purposes.

Phlegraean Fields volcanism includes both continental (*Campi Flegrei s.s.*) and insular (*Ischia and Procida* Islands) activity. The oldest outcropping products belong to *Ischia* activity (150 Ka; Poli et al., 1987; Vezzoli, 1988), while as concern continental volcanism, the first activity is dated back to 58 Ka (<sup>40</sup>Ar/<sup>39</sup>Ar, Pappalardo et al., 1999). It is also divided by means of two volcanic events, the most important in terms of thickness and areal distribution. The first large eruption is represented by Campanian Ignimbrite deposits (39 Ka; Fedele et al., 2008), the second one is the Neapolitan Yellow Tuff (therefore NYT, 15 Ka; Deino et al., 2004). Both events are the main chronostratigraphic markers for the reconstruction of the Phlegraean volcanic district.

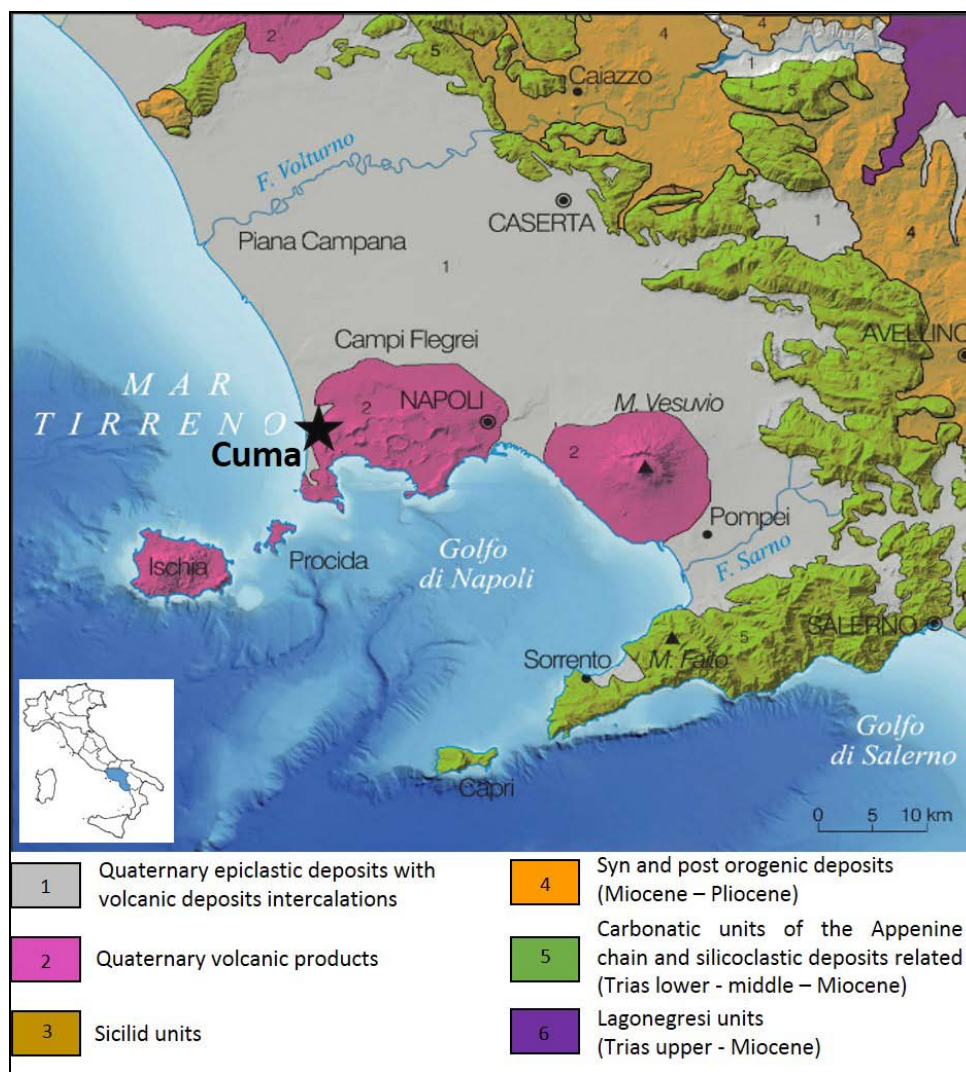


Figure 1. Geological sketch map of the Bay of Naples area with location of Cuma site. ([http://www.isprambiente.gov.it/Media/carg/447\\_NAPOLI/Foglio.html](http://www.isprambiente.gov.it/Media/carg/447_NAPOLI/Foglio.html), modified).

These deposits, linked to high-magnitude explosive eruptions, were accompanied by caldera collapse followed by emplacement of pyroclastic sequences (Orsi et al., 1996; Perrotta et al., 2006; Melluso et al. 2012 and references therein). The last eruption of Phlegraean Fields dates back to 1538 AD (*Monte Nuovo*) but the volcanic activity still carries on, as testifies by recent bradyseismic episodes and intense fumarolic activity.

The Phlegraean products range from shoshonitic basalt through latite, to trachyte, trachyphonolite and phonolite. The most common mineral phases are clinopyroxene, plagioclase, sanidine, biotite and magnetite with rare olivine. The accessory minerals are zircon, brown amphibole and titanite, whereas nepheline and exotic minerals (e.g. disilicates) can be found in most evolved products (Morra et al. 2010 and references therein; Melluso et al. 2012).

The Somma-Vesuvius central volcanic complex, is located in the southern part of Campanian Plain (Fig. 1). It is a stratovolcano formed by the oldest strato-

cone of Mount Somma, in which Vesuvius cone formed as consequence of 79 AD eruption ("*Pompei*"; e.g., Cioni et al., 1999; Rolandi et al., 1998, 2004). The Somma-Vesuvius volcanism showed a cyclic mechanism in which periods of quiescence were interrupted by plinian or subplinian eruptions (Rolandi et al., 1998). The last eruption dates back to 1944. The Somma-Vesuvius volcanic rocks vary from potassic to ultrapotassic, with degree of alkalinity and thus silica-undersaturation increasing with time.

These two volcanic complex rest on the Campanian Plain, a structural depression, bordered by Meso-Cenozoic carbonates forming the Southern Apennine chain to the N/E, the Sarno Mountains to the E, and Monti Lattari ridge to the S (Fig. 1).

### 3. THE ARCHAEOLOGICAL SITE

The archaeological site of Cuma (Campanian Region, southern Italy), includes also the *Necropolis* area located outside the *Porta Mediana*, one of the main gates of the ancient city. The funerary site is

divided in several sectors among which D46 represents one of the most interesting (Fig. 2). Excavated in 2012, it includes the D46b funerary complex (1<sup>st</sup> century BC), and later buildings, ranging in time from 2<sup>nd</sup> and 3<sup>rd</sup> century AD. It is set along the Eastern boundary of a square outside the city gate, in a strategic location to understand the chronological evolution of the *Porta Mediana* site (Fig. 2; Brun et al.,

2013). The D46b funerary monument, slightly trapezoidal in shape and built in *opus quasi-reticulatum*, is not entirely preserved. The only original building is the burial chamber, probably semi-hypogean (Fig. 3). All the walls are built against earth, so the chamber does not have exterior facings, while its inner part is covered by plaster.

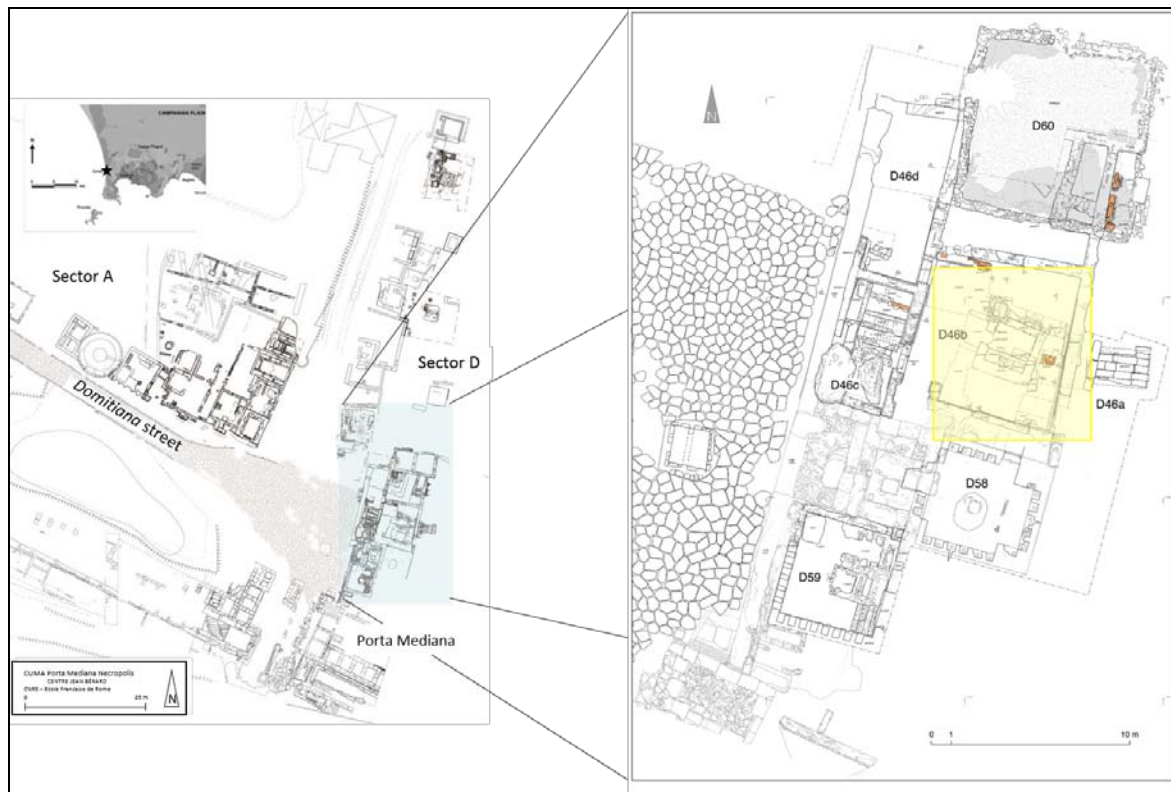


Figure 2. Cuma, sketch map of *Porta Mediana* Necropolis (modified after Covolan & Lemaire, 2017) with the detail of northeastern area of the Gate, which includes the investigated D46b funerary monument (yellow color).

The stratigraphic excavation allowed identifying at least two building phases corresponding to different intended use of the funerary monument.

To the first phase belong semi-circular structures in *opus incertum* made of yellow tuff bound with grey mortar, in which some niches, probably for cinerary urns, were carved. During the second phase the funerary room has undergone some transformations, including the construction of two funerary bed in replacement of urns along with the addition of partially preserved *cocciopesto* flooring.

During the 1<sup>st</sup> century AD at least three others tombs, today obliterated, were built within the sector. Between the end of the 1<sup>st</sup> century and the first decades of the 2<sup>nd</sup> century AD, the area underwent

several transformations, including the realization of the *Domitiana* street and the monumentalization of the space in front of the Gate. Moreover, funerary buildings belonging to the previous phases were destroyed and a short time later a new public building is built along the eastern edge of the paving-stones area in front of the *Porta Mediana*. The latter consists of a monumental facade and some commercial buildings (Brun & Munzi, 2013).

From the middle of the 3<sup>rd</sup> century AD the area is progressively abandoned, while during the 6<sup>th</sup> century AD it becomes a source of building materials, in which marbles were used for lime production (Covolan & Lemaire, 2017).



Figure 3. Cuma, D46b funerary monument.

#### 4. MATERIALS AND METHODS

Eleven samples of mortars were collected from boundary masonries belonging to different building times ranging from 1<sup>st</sup> century BC to 3<sup>rd</sup> century AD, (Fig. 4; Tab. 1). They can be divided in two typolo-

gies: bedding and coating mortars. The first type includes six samples taken from *opus quasi-reticulatum* masonries; the coating mortars are represented by five samples of multi-layer covering (Tab. 1).

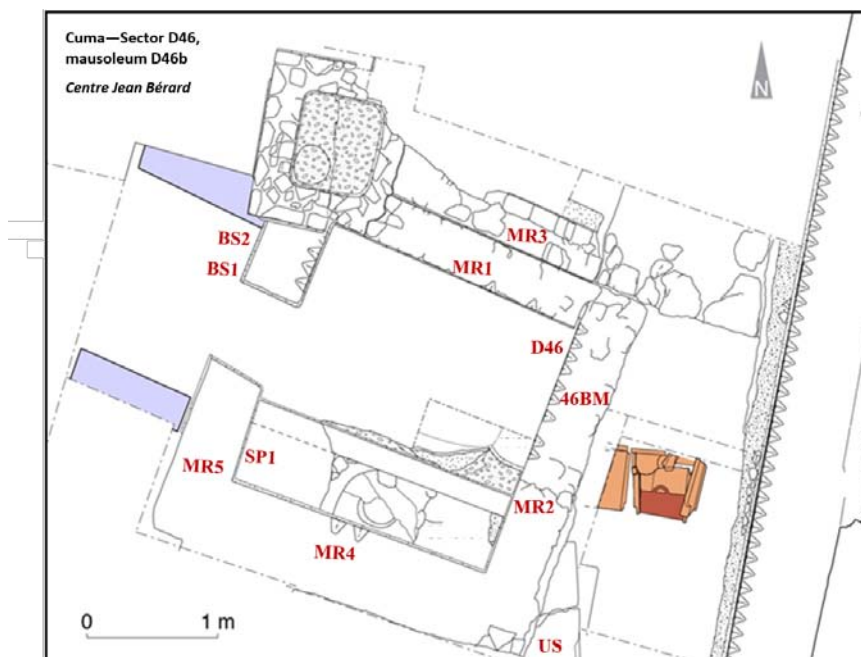


Figure 4. Mortars sampling points from D46 sector and D46b mausoleum. Surveyed by G. Chapelin, CJB/CNRS.

Instrumental methods included: 1) Optical Microscopy (OM) on thin sections; 2) X-Ray powder Diffraction (XRPD); 3) Scanning Electron Microscopy and Energy Dispersive X-ray spectroscopy (SEM-EDS) analyses. All the analyses were performed at DiSTAR laboratories, University of Naples Federico II.

Optical microscopy was carried out by Leitz Laborlux 12 pol, in order to study composition and texture of the mortar (Elsen, 2005; UNI-EN 11305:2009

and UNI-EN 11176:2006). Images were captured by digital videocamera "Leica DFC 280".

X-Ray powder diffraction was carried out by Panalytical X'Pert Pro diffractometer equipped with a RTMS X'Celerator detector (CuK $\alpha$  radiation, 40 kV, 40 mA, 2 $\theta$  range from 4° to 70°, equivalent step size 0,017° 2 $\theta$ , 30 s per step counting time) both on binder and aggregate, mechanically separated after powdered sample by hand, in order to preserve soluble

phases, following the UNI 11305 recommendations, in an agate mortar. Identification of mineral phases was performed by Panalytical Highscore Plus 3.0e software with ICSD database.

SEM-EDS analyses were performed on not altered *juvenile* fragments from thin sections to distinguish the nature of aggregate and determine chemical composition of mortar binder. An Energy Dispersive Spectrometer (JEOL JSM-5310 microscope and an Oxford Instruments Microanalysis Unit, equipped with an INCA X-act detector and operating at 15 kV primary beam voltage, 50-100 mA filament current, vari-

able spot size, from 30,000 to 200,000x magnification, 20 mm WD and 50 s net acquisition real time) was employed referring to Guarino et al. (2017) and references therein. Measurements were made with an INCA X-stream pulse processor and with INCA Energy software. The following standards were used for calibration: diopside (Ca), San Carlos olivine (Mg), anorthoclase (Al, Si), albite (Na), rutile (Ti), fayalite (Fe), Cr<sub>2</sub>O<sub>3</sub> (Cr) rhodonite (Mn), orthoclase (K), apatite (P), fluorite (F), barite (Ba), strontianite (Sr) and sodium chloride (Cl). Backscattered electron (BSE) images were obtained with the same instrument.

Table 1. Type of sampled mortars.

| SAMPLE | TYPE    | PERIOD   |
|--------|---------|--|
| MR1    | bedding | 2 <sup>nd</sup> half of 1 <sup>st</sup> century BC |
| MR2    | bedding | 2 <sup>nd</sup> half of 1 <sup>st</sup> century BC |
| MR3    | coating | 2 <sup>nd</sup> half of 1 <sup>st</sup> century BC |
| MR4    | coating | 2 <sup>nd</sup> half of 1 <sup>st</sup> century BC |
| MR5    | coating | 2 <sup>nd</sup> half of 1 <sup>st</sup> century BC |
| US     | bedding | 1 <sup>st</sup> century BC                         |
| SP1    | bedding | 2 <sup>nd</sup> half of 1 <sup>st</sup> century BC |
| D46    | coating | 2 <sup>nd</sup> half of 1 <sup>st</sup> century BC |
| 46BM   | bedding | 2 <sup>nd</sup> half of 1 <sup>st</sup> century BC |
| BS1    | bedding | 2 <sup>nd</sup> - 3 <sup>rd</sup> century AD       |
| BS2    | coating | 2 <sup>nd</sup> - 3 <sup>rd</sup> century AD       |

## 5. RESULTS

### 5.1 Optical microscopy

Optical microscopy was carried out on all mortar samples to obtain qualitative information about the mix-design of lime-based mortars and their aggregate.

Bedding mortars (MR1, MR2, SP1, BS1, US, 46BM samples) are characterized by a mixture of light olive grey (5Y 6/2 Munsell) lime matrix and volcanic aggregate. The aggregate/binder ratio, observed in all thin sections always exceeds the 50%, according Normal 11176:2006. Aggregate is poorly sorted (Gagliardi et al., 1980) with medium-low rounded clasts (Krumbein & Sloss, 1979), ranging in size from fine (less than 2 mm) to coarse grained (up to 7 mm

in size), consisting of pyroclastic fragments, such as pumice (sometimes with sanidine and clinopyroxene) and obsidian, and subordinate crystal-clasts of sanidine, clinopyroxene, plagioclase and mica (Fig. 5a). Lime lumps occur in almost all samples, except in BS1 and MR1; in this latter, as well as in the MR2 sample carbonate clasts are also identified (Fig. 5b).

Coating mortars are composed by different layers, shown in table 2, along with relative thicknesses.

Coating mortars (MR3, MR4, MR5, BS2, D46 samples) are composed at least by two layers: the innermost (layer 0), representing the anchorage layer, also named scratch layer, followed by layer 1 (*arriccio*) (Izzo et al., 2016 and references therein).

Table 2. Stratigraphy of mortar sample with thickness of identified layers

|     | Anchorage | Arriccio | Plaster | Painting         |
|-----|-----------|----------|---------|------------------|
| MR3 | 6 mm      |          | 1.6 mm  |                  |
| MR4 | 5 mm      | 3 mm     |         |                  |
| MR5 | 9 mm      | 3 mm     |         |                  |
| BS2 | 8 mm      | 2 mm     |         |                  |
| D46 | 5 mm      |          | 0.8 mm  | 39 µm and 105 µm |

Anchorage layers show 2.5Y 7/3 (Munsell) colored matrix, mixed mainly with volcanic aggregate. Matrix shows from cryptocrystalline to micritic texture, generally deriving from pozzolanic reaction between binder and aggregate. The aggregate/binder ratio ranging from 40% (D46) to 50% (MR4, MR5, BS2). The aggregate is ranging in size from fine (2µm) to coarse

grained (up to 13 mm), except for D46 sample, showing predominant fine grain size. Shape of the anchorage layer aggregate mostly varies from sub-angular to sub-rounded (Krumbein & Sloss, 1979) with poorly sorted size distribution (Gagliardi et al., 1980). The thickness of this layer ranges from 5 mm (MR4 and D46) to 9 mm (MR5).

Volcanic aggregates are characterized, in order of abundance, by pumice (sometimes with alkali feldspar and clinopyroxene) and obsidian (fragments), along with sanidine, clinopyroxene, plagioclase and brown mica grain. Crystal fragments are particularly abundant in MR5 and MR4 samples (Fig. 5c) comparing to the anchorage layer of MR3, D46 and BS2 samples (Fig. 4d). Subspherical or elongated lime lumps, ranging from 200  $\mu\text{m}$  to 4 mm, with well-defined edges, are often observed in the matrix. Shrinkage cracks (in the middle area), are also observed (Fig. 5e). Calcareous clasts occurrence was detected in MR3, D46 and BS2 samples.

The transition to *arriccio* (layer 1) is well marked in all coating mortars (except in BS2 samples, in which well-defined layers cannot be identified, Fig. 5d), also for the occurrence of few ceramic fragments and volcanic aggregates in subordinate amount with respect to layer 0.

The *arriccio* layer can be recognizable in BS2, MR5 and MR4 samples. It can be distinguished from anchorage layer mainly for the features of aggregate. In this layer, the aggregate is less abundant compared to layer 0 (about 40%), ranging in size from fine grained

(less than 2 mm) to a maximum of 3 mm (MR5 sample). It appears moderately sorted (Krumbein & Sloss, 1979) with medium roundness of grains (Gagliardi et al., 1980), also revealing occurrence of ceramic fragments (Fig. 5f). The thickness of this layer range from 3 mm (MR4 and MR5) to 2 mm (BS2).

The complete stratigraphic sections, which should include both preparation (plaster) and finishing (painting) layers, are not preserved in all samples. Among investigated coating mortars only two samples show this kind of layers: D46 and MR3 (Fig. 5g, h). In both samples *arriccio* layer is lacking, while a thick layer (0.8-1.6 mm for D46 and MR3, respectively) of plaster can be easily distinguished. The main differences between these two samples regard: a) occurrence of calcareous aggregate (maximum grain size 2  $\mu\text{m}$ ); b) presence of shells, identified only in MR3 sample.

As concern outermost layers, D46 sample shows two preparations (layers 2 and 3), very similar from petrographic point of view and characterized by carbonate dense binder, with thickness of 39  $\mu\text{m}$  and 105  $\mu\text{m}$ , respectively. Instead, the MR3 sample has only a very thin paint finishing layer.

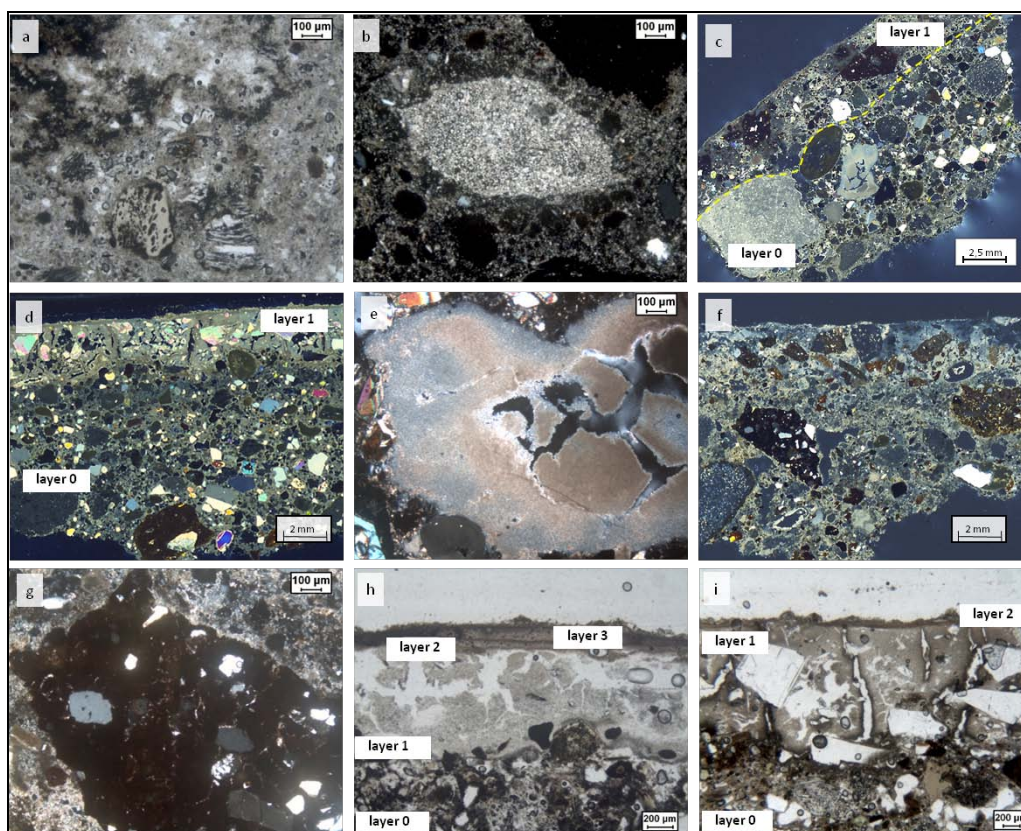


Figure 5. Representative images of: a) volcanic fragments, US, (PPL); b) carbonate fragments, US (CPL); c) abundant crystal fragments in anchorage layer, MR5 sample (thin section scan); d) low amount of crystal fragments in anchorage layer, MR3 sample (thin section scan); e)  $\text{CaCO}_3$  lime lump showing shrinkage cracks, D46 (CPL); f) ceramic fragments in *arriccio* layer, MR5 (CPL); g) undefined layers in the BS2 sample (thin section scan); h) anchorage, plaster and two preparation layers, D46 (PPL) i) anchorage, plaster anchorage, plaster with calcareous aggregates and paint finishing layer MR3 (PPL).

PPL: Parallel Polarized Light; CPL: Cross Polarized Light.

## 5.2 X-ray powder diffraction

XRPD results confirmed occurrence of lime-based mortar with volcanic aggregate, as shown by semi-quantitative analyses reported in Table 3, in which aggregate and binder are identified by the A and B at the end of the abbreviation, respectively.

Calcite is the most abundant binder phase, even if a subordinate amount could be derived also from calcareous clasts not well separated during the mechanical grinding. Sanidine, mica-group minerals and subordinate analcime were detected in all samples. Phillipsite was recognized, in small amounts, in many samples (except in BSP1B and MR2B). Plagioclase only occurs in three samples: BSP1B, MR2B and USB. Small amount of quartz was also detected in

BS2B sample. Finally, vaterite, a calcium carbonate polymorph, metastable under ambient conditions, was observed in MR2B and MR4B samples. Its occurrence is probably related to a) alteration of carbonate binder, which stabilizes in the presence of organic compound or b) formed as an alteration product of C-A-S-H (hydraulic binder) in both subaerial and submarine environments (Brandon *et al.*, 2014).

XRPD analyses also highlight calcite as the main component of the aggregate (Table 3). However, its presence might be related to the binder fraction remained in contact with aggregate fragments, as consequence of mechanical separation.

**Table 3. Semi-quantitative mineralogical analyses (XRPD) of binder and aggregate samples: ++++ predominant, +++ abundant, ++ moderate, + scarce. Mineral abbreviations from (Siivola & Schmid, 2007; Whitney & Evans, 2010).**

| BINDER    |      |      |    |     |     |     |     |     |     |    |     |
|-----------|------|------|----|-----|-----|-----|-----|-----|-----|----|-----|
|           | cal  | sa   | pl | mca | php | cbz | anl | vtr | qtz | px | hem |
| BS1B      | ++++ | ++   |    | +   | +   |     | +   |     |     |    |     |
| BS2B      | ++++ | ++   |    | +   | +   | +   | +   |     | +   |    |     |
| BSP1B     | ++++ | ++   | +  | +   |     |     | +   |     |     |    |     |
| BMB       | ++++ | +++  |    | +   | +   |     | +   |     |     |    |     |
| MR1B      | ++++ | ++   |    | ++  | +   |     | +   |     |     |    |     |
| MR2B      | +++  | ++   | +  | +   |     |     | +   | ++  |     |    |     |
| MR3B      | +++  | +++  |    | ++  | +   |     | +   |     |     |    |     |
| MR4B      | ++++ | ++   | +  | +   | +   |     | +   | ++  |     |    |     |
| MR5B      | +++  | ++   | +  | +   | +   |     | +   |     |     |    |     |
| 46BB      | ++++ | ++   | +  | +   | +   |     | +   |     |     |    |     |
| USB       | ++++ | +++  | ++ | ++  | +   |     | +   |     |     |    |     |
| AGGREGATE |      |      |    |     |     |     |     |     |     |    |     |
| BS1A      | ++++ | ++   |    | +   | +   | +   | +   |     |     |    |     |
| BS2A      | ++++ | ++   |    | +   | +   | +   | +   |     |     |    |     |
| BSP1A     | ++++ | ++   | ++ | +   | +   |     | +   |     |     |    |     |
| BMA       | ++++ | ++   |    | +   | +   |     | +   |     |     |    |     |
| MR1A      | ++++ | ++   | ++ | ++  | +   |     | +   |     |     |    |     |
| MR2A      | +++  | +    |    | ++  |     | +   |     | +++ |     |    |     |
| MR3A      | ++++ | ++   | ++ | +   | +   |     | +   |     |     |    |     |
| MR4A      | +++  | ++   | ++ | +   | +   | +   | +   | ++  |     |    |     |
| MR5A      | ++++ | ++   | ++ | +   | +   | +   | +   |     |     |    |     |
| 46BA      | +++  | +++  | ++ | ++  | ++  | +   | +   |     |     |    |     |
| USA       | ++++ | ++++ | ++ | +   | ++  | +   | +   |     |     |    |     |
| BS2C      | +++  | +    | ++ | +   |     |     |     |     | +++ | +  | +   |

cal: calcite; sa: sanidine; pl: plagioclase; mca: mica; php: phillipsite; cbz: chabazite; anl: analcime; vtr: vaterite; qtz: quartz; px: pyroxene; hem: hematite.

Only for MR2 and MR4 mortars, both in aggregate and binder samples (MR2A, MR2B, MR4A and MR4B), XRPD results highlight the presence of

vaterite, along with calcite, sanidine, chabazite, phillipsite (MR4A), plagioclase (MR4) and mica.

Concerning ceramic fragments from BS2C sample, they are mainly composed by calcite, quartz and, subordinately, by plagioclase, sanidine, pyroxene, mica and hematite.

X-ray patterns also suggest presence of a Low Ordered or Amorphous Phase (LO-AP), that may be related to volcanic glass components (*juvenile* fragments) and hydraulic phases (C-A-S-H; Jackson et al., 2010) formed after pozzolanic reactions between lime and volcanic glasses or *cocciopesto* grains (obtained crushing shattered tiles, brick and pottery;

Fernandez et al., 2010; Middendorf et al., 2005; Izzo et al., 2016).

### 5.3 Electronic microscope observation and chemical analyses of minerals

SEM-EDS observations performed on the binder allow to identify some phases characterized by 'spongy' morphology (García et al., 2009; Fernández et al., 2010) that highlight, as suggest by XRPD results, the formation of a newly hydraulic phases (C-A-S-H; Fig. 6), attesting the reaction between lime and pozzolanic materials.

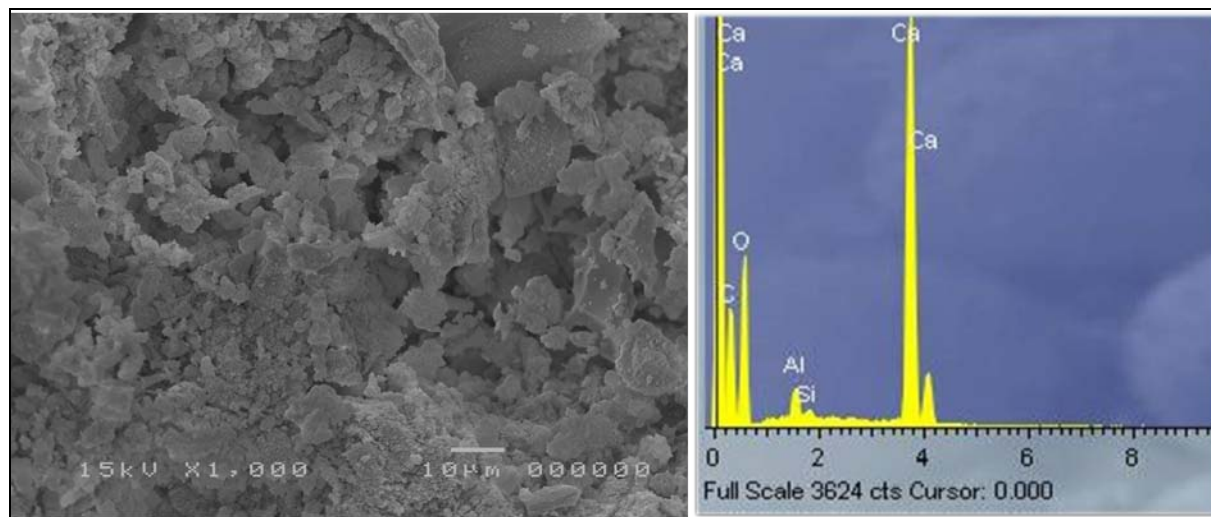


Figure 6. SEM image and relative EDS spectrum of neo-formed hydraulic phases (C-A-S-H), BS1 sample.

As regards aggregate, SEM-EDS analyses, according to XRPD data, once again evidence the presence of phillipsite with well-defined prismatic crystal

habit and of pseudocubic crystals of chabazite, often associated with acicular crystals of phillipsite (Fig. 7; de' Gennaro et al., 1999).

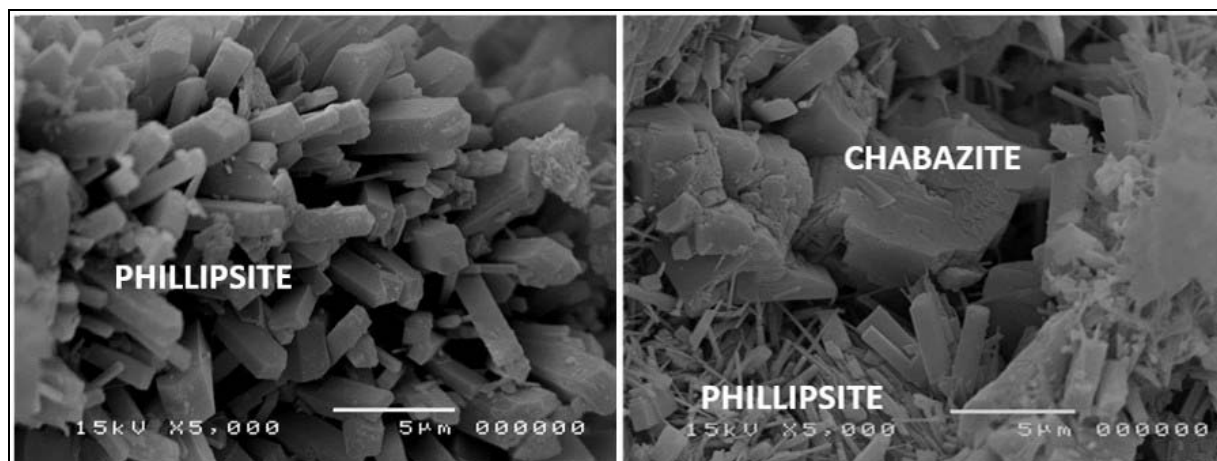


Figure 7. SEM image of phillipsite (on left) and chabazite (on right) crystals from MR1 sample.

In order to infer provenance of volcanic aggregate, SEM-EDS microanalysis was carried out on fresh *juvenile* fragments (Fig. 7, Table 4). Investigations were performed on three points for each pumice. The occurrence of many altered pumice required a

careful selection of analyses closing between 98% and 100%, to exclude altered ones.

Chemical classification (TAS diagram, according to Le Maitre et al., 1989) of investigated pumice shows a trachytic/phonolitic composition ( $\text{SiO}_2 = 59.6\text{-}63.9$  wt.%;  $\text{Na}_2\text{O}+\text{K}_2\text{O} = 12.4\text{-}13.7$  wt.%; Fig. 9)

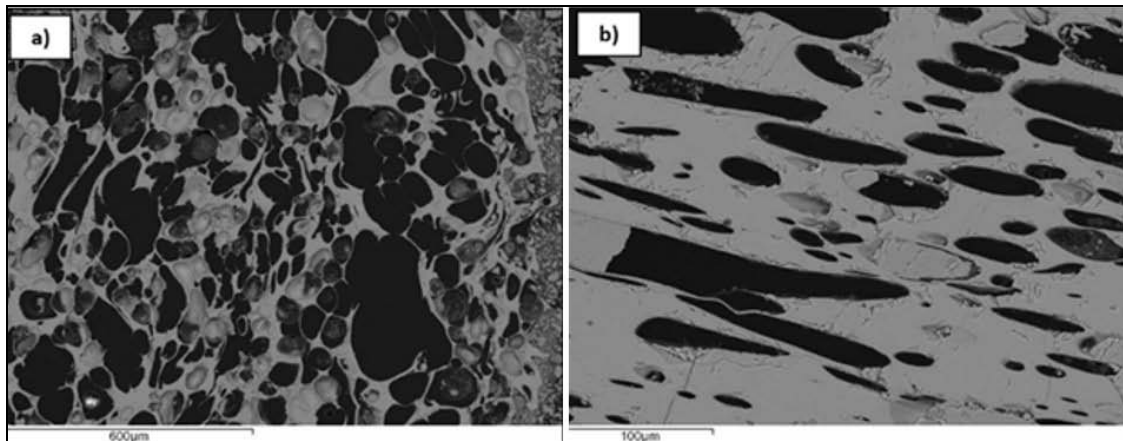


Figure 8. Back Scattered-SEM images of pumice from a) MR1 and b) BS1 samples.

Table 4. Major element concentrations (wt.%, by EDS), pumice.

| wt%                            | MR1a   | MR1b   | MR3    | MR4    | MR5    | SP1    | BS1    | BS2    | US     | 46BM   | D46    |
|--------------------------------|--------|--------|--------|--------|--------|--------|--------|--------|--------|--------|--------|
| SiO <sub>2</sub>               | 61.6   | 60.3   | 60.2   | 63.2   | 62.0   | 60.0   | 59.6   | 63.9   | 63.9   | 63.2   | 61.6   |
| TiO <sub>2</sub>               | 0.43   | 0.82   | 0.33   | 0.50   | 0.12   | 0.82   | 0.70   | 0.55   | 0.49   | 0.11   | 0.36   |
| Al <sub>2</sub> O <sub>3</sub> | 18.3   | 18.0   | 18.0   | 18.2   | 17.9   | 18.5   | 18.2   | 18.1   | 17.2   | 17.7   | 18.2   |
| Fe <sub>2</sub> O <sub>3</sub> | 2.45   | 3.06   | 2.90   | 2.34   | 3.18   | 2.60   | 3.50   | 3.20   | 2.31   | 2.61   | 2.70   |
| MnO                            | 0.13   | 0.07   | 0.20   | 0.12   | 0.00   | 0.05   | 0.21   | 0.35   | 0.09   | 0.26   | 0.35   |
| MgO                            | 0.37   | 0.45   | 0.25   | 0.24   | 0.49   | 0.51   | 0.57   | 0.47   | 0.31   | 0.27   | 0.19   |
| CaO                            | 2.21   | 2.20   | 2.60   | 1.72   | 2.28   | 2.24   | 2.53   | 2.31   | 1.50   | 1.39   | 2.00   |
| Na <sub>2</sub> O              | 4.40   | 4.50   | 4.40   | 4.54   | 3.89   | 4.29   | 4.35   | 3.67   | 5.96   | 5.74   | 4.86   |
| K <sub>2</sub> O               | 8.72   | 8.72   | 9.30   | 8.57   | 8.99   | 9.32   | 8.77   | 8.73   | 6.97   | 7.07   | 8.45   |
| P <sub>2</sub> O <sub>5</sub>  | 0.08   | 0.23   | 0.30   | bdl    | bdl    | 0.36   | 0.22   | 0.26   | bdl    | 0.07   | 0.12   |
| SO <sub>3</sub>                | 0.07   | 0.07   | 0.10   | 0.17   | 0.02   | bdl    | 0.30   | 0.18   | 0.18   | 0.22   | 0.04   |
| BaO                            | 0.21   | bdl    | 0.30   | bdl    | 0.28   | bdl    | bdl    | bdl    | 0.20   | 0.19   | bdl    |
| SrO                            | 0.18   | 1.09   | 0.60   | bdl    | 0.21   | 0.82   | 0.48   | 0.67   | 0.83   | bdl    | 0.46   |
| Cl <sup>-</sup>                | 0.81   | 0.51   | 0.70   | 0.53   | 0.70   | 0.53   | 0.62   | 0.57   | bdl    | 0.83   | 0.76   |
| F <sup>-</sup>                 | bdl    | bdl    | bdl    | bdl    | bdl    | bdl    | bdl    | bdl    | bdl    | 0.29   | bdl    |
| Total                          | 100,00 | 100,00 | 100,00 | 100,00 | 100,00 | 100,00 | 100,00 | 100,00 | 100,00 | 100,00 | 100,00 |
| NaO+K <sub>2</sub> O           | 13.1   | 13.2   | 13.7   | 13.1   | 12.9   | 13.6   | 13.1   | 12.4   | 12.9   | 12.8   | 13.3   |

bdl: below detection limit

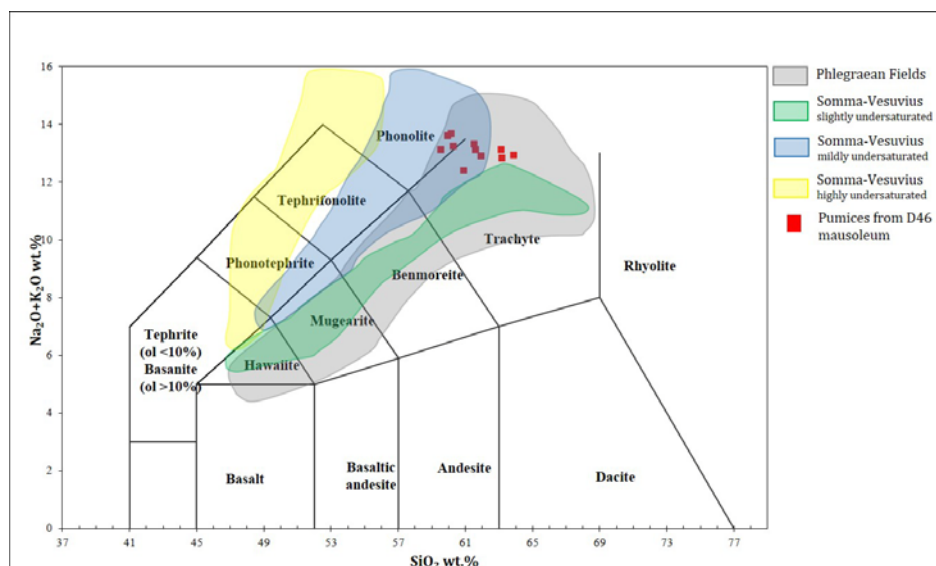


Figure 9. Classification of pumice fragments from D46b funerary monument samples according to the TAS diagram (Le Maitre et al., 1989). Compositional fields of Phlegraean Fields and Somma-Vesuvius products and volcanic glasses are also reported (data from Morra et al., 2010 and references therein; figure modified after De Bonis et al., 2016).

## 6. DISCUSSION

The study allowed to characterize several mortars belonging to D46 sector.

The obtained chemical and mineralogical results, combined with archaeological data, provide significant information about the D46 bedding (MR1, MR2, US, SP1, 46BM, BS1) and coating (MR3, MR4, MR5, D46, BS2) mortars samples. Although the existence of different typologies already testifies the high knowledge and skill of Roman craftsmen, only a detailed investigation allowed to point out the provenance of raw materials and used technology.

### 6.2 Provenance

Coating and bedding mortars were made by a mixture of lime with three different aggregate types: limestone, volcanic sand, ceramic fragments, these latter used only for coating purposes.

As regard limestone, mainly used for binder and aggregate, is not possible precisely to assign this material to specific formation. However, it is reasonable to hypothesize that this geomaterial comes from Mesozoic limestone outcrops that border *Campania* Plain (Fig. 1).

Aggregate has predominantly a volcanic origin and it mainly consists of *juvenile* products (i.e.: pumice, scoriae and obsidian fragments), along with crys-

talline phases, such as sanidine, clinopyroxene, plagioclase and brown mica crystal clasts. Local source of volcanic aggregate is firstly suggested by the location of *Necropolis* within Phlegrean Fields area (Fig. 1; 10), in which volcanic material (tuffs) have been widely exploited as aggregates mixed with *pozzolana* and lime to obtain mortars since Roman times (Vitruvio, *De Architectura*). Moreover, the result of mineralogical analyses carried out on volcanic aggregate highlighted the presence of phillipsite, chabazite and analcime, the typical zeolitic association of Phlegrean tuffs, namely Neapolitan Yellow Tuff (NYT) and Campanian Ignimbrite-Yellow *facies* (de Gennaro et al., 2000; Langella et al., 2013). This evidence is also confirmed by the chemical analysis of pumice fragments that, according to the TAS diagram, follow the compositional trend of rocks from Phlegrean Fields (Fig. 9). A further and more specific indication might come from previous studies performed on *Piscina Mirabilis* and Thermal Complex of *Baia*, two Phlegrean archaeological sites (Rispoli et al., 2015; 2016), pointing out that in these site mortars were obtained by mixing lime with volcanic aggregate from NYT deposit. Moreover, such hypothesis could be consistent with the occurrence of NYT outcrops close to the city of *Cuma* (Fig. 10).

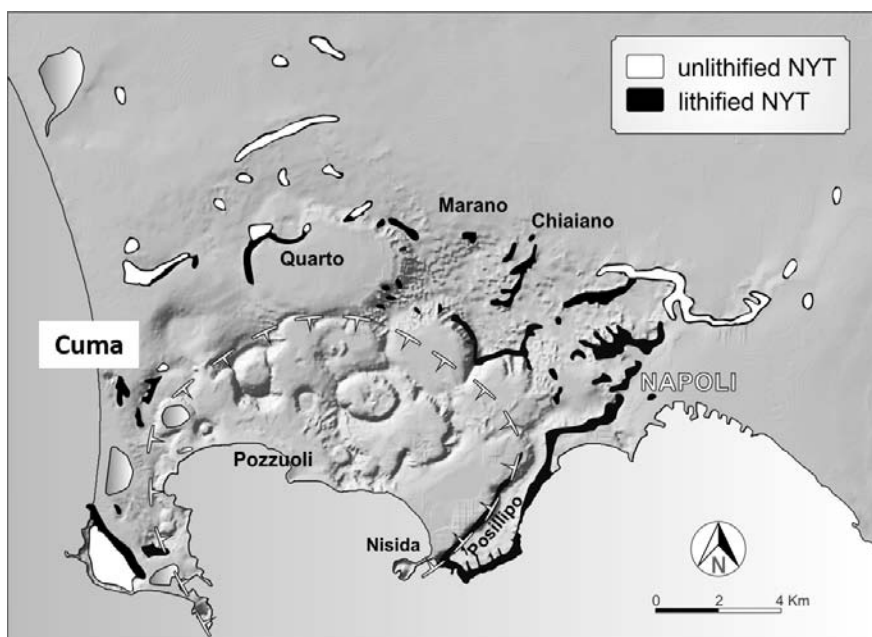


Figure 10. Lithified and unlithified NYT deposits within Phlegrean Fields area, modified after Colella et al., 2017.

All the results highlight that no significant differences occurred in terms of composition between bedding and coating mortars, except for the presence, in the latter, of ceramic fragments, probably used in addition to pumice to improve pozzolanic reactions.

### 6.3 Technology

As regards production techniques, the bedding and coating mortars are lime-based with addition of pozzolanic materials, according to Vitruvius' recipe (*De Architectura*), sometimes along with *cocciopesto*.

Lime lumps are common within binder. They represent unreacted lime related to dry-slaking process. Along with lime lumps, carbonate aggregates were found and linked to incomplete decarbonation processes during lime production, probably due to low temperature or insufficient calcination time (Bakolas et al. 1995; Barba et al., 2009; Yaseen et al., 2012). The occurrence of both lime lumps and carbonate aggregates testifies for a not accurate mortars manufacturing technology.

Further information about used technology come from the identification, by means of EDS-SEM analyses, of newly formed hydraulic phase, the gel-C-A-S-H. These hydrated calcium and aluminium silicates could derive from reaction between silica and aluminium contained in the "pozzolanic" material (volcanic and ceramic fragments) commonly added to the mix design.

However, not many information about these manufacturing techniques has been so far reported in literature data (Drdacky et al., 2013).

Bedding mortars result from a mixture of slaked lime, fine to coarse-grained volcanic fragments and carbonate rocks. Coating mortars are result from a mixture of slaked lime, fine grained volcanic, ceramic and carbonate aggregates.

Moreover, as concern the coating mortars, they have been using a multi-layered technique, which, from the inner to the outer, has provided: anchorage, *arriccio*, plaster and preparation layer. Each layer shows different features, depending on its purpose.

The anchorage layer, the innermost, is made by poorly sorted and rounded volcanic aggregate (mainly pumice and obsidian) embedded in a carbonate matrix. The scratchy fabric of the anchorage layer ensures the good adhesion to the wall, making easy the '*arriccio*' application. The *arriccio* layer shows less abundant aggregate with respect to the anchorage layer. The aggregate, moderately sorted with medium roundness, is characterized by ceramic fragments that, as *pozzolana*, also provide further strength to the mortars-based too. This layer anyway is not present in all investigated samples.

The plaster and preparation layers, not always well preserved, are characterized by lower amount of aggregate (mostly with carbonate composition). The preparation layer shows a finest grain size and a reduced porosity more suitable for following painting layers.

## 7. CONCLUSIONS

The research pointed out new insights about technological performances of Roman craftsmen, pro-

ducing different mortars from D46 funerary monument.

Results were obtained combining chemical, mineralogical and archaeological data with the aim of: 1) characterized the used mix-design, 2) identify raw materials, 3) improve the knowledge on manufacturing techniques in Roman time.

The location of the Necropolis in the Phlegrean Fields granted craftsmen a large amount of geomaterials, widely used for mortar preparation. Indeed, in both types of mortars (bedding and coating), the use of volcanic materials of local origin has been recognized.

Investigated mortars, though produced over a wide period of time, show continuity in the choice of materials and used technology.

All lime-based mortars, with addition of volcanic aggregate (pumice, obsidian, lithic, and crystal fragments of alkali feldspar, plagioclase, pyroxene and mica), suggesting that mix design was obtained by mixing lime and volcanic phlegrean products. The use of the Neapolitan Yellow Tuff is strongly suggested by the characteristic mineral assemblage (phillipsite, cabasite and analcime), and also by the presence of a tuff cone relict (*Monte Grillo*) very close to *Necropolis*.

However, no sufficient elements allow to exclude also the use of Campanian Ignimbrite yellow *facies*, characterized by a mineralogical composition very similar to the Neapolitan Yellow Tuff one.

The limestone, used for both binder production and as main aggregate (coating mortars and preparation layers), may have been quarried from carbonate rocks that surround the Campanian Plain.

As far as production techniques are concerned, detailed information arises from coating mortars. In fact, although the innermost anchoring mortars (scratch layers) show presence of lime lumps, associated with defects in production technique, multiple layering allows to hypothesize a good knowledge by craftsmen of geomaterials and their properties.

Such good knowledge is further confirmed by the choice of a) coarse grain size for the aggregate of the anchoring layer and b) addition of ceramic fragments, which provide additional pozzolanic effect.

New data deriving from the study of these Roman mortars may represent a significant contribution to the knowledge of the ancient, but surprisingly actual, constructive techniques.

This research is also the starting point for comparing mortars from numerous funerary monuments of the same site with the aim of reproducing mortars of high durability and/or finding suitable restoration materials.

## ACKNOWLEDGEMENTS

The authors wish to thank Dott. Roberto de Gennaro for his kind support in electron-microprobe determinations and backscattered electron images and Dott. Sergio Bravi for his technical ability in thin sections preparation. This research was granted by national research project PON "SINAPSIS" (Sistema Protezione Siti Sensibili - PON01\_01063).

## REFERENCES

- Aloise, P., Ricca, M., La Russa, M.F., Ruffolo, S.A., Belfiore, C.M., Padeletti, G., Crisci, G.M. (2013). Diagnostic analysis of stone materials from under water excavations: the case study of the Roman archaeological site of Baia (Naples, Italy). *Applied Physics A: Materials Science and Processing*, Vol. 114, pp. 655-662. doi: 10.1007/s00339-013-7890-1.
- Bakolas A., Biscontin G., Contardi V., Franceschi E., Moropoulou A., Palazzi D. and Zendri, E. (1995). Thermoanalytical research on traditional mortars from Venice. *Thermochimica Acta* Vol. 269/270, pp. 817-828. doi: 10.1016/0040-6031(95)02574-X.
- Barba, L., Blancas, J., Manzanilla, L. R., Ortiz, A., Barca, D., Crisci, G. M., Miriello, D., Pecci, A. (2009). Provenance of the limestone used in Teotihuacan (Mexico): a methodological approach. *Archaeometry*, Vol. 51, pp. 525-545. doi: 10.1111/j.1475-4754.2008.00430.
- Bonazzi A., Santoro S., Mastrobattista E. (2007). Caratterizzazione archeometrica delle malte e degli intonaci dell'Insula del Centenario. In: Pompei. Insula del Centenario (IX,8). I. Indagini diagnostiche geofisiche e analisi archeometriche, Ed. Ante Quem pp. 93-128.
- Brandon C., Hohlfelder R.L., Jackson M.D., Oleson J.P. (2014). *Building for Eternity: The History and Technology of Roman Concrete Engineering in the Sea*. Oxford Books.
- Brun J. P., Munzi P. (2008). La necropoli romana della Porta Mediana. In F. Zevi, F. Demma, E. Nuzzo, C. Rescigno, C. Valeri (éd.), Museo archeologico dei Campi Flegrei. Catalogo generale. 1. Cuma, Napoli, pp. 396-399.
- Brun J.P., Munzi P., Cavassa L., Chapelin G., Cormier A., Duday H., Gualandi S., Le Berre S., Lemaire B., Meluziis N., Neyme D., Piffeteau J.M., Watel A. (2013). « Cumes », *Chronique des activités archéologiques de l'École française de Rome [En ligne], Italie du Sud*, mis en ligne le 28 juin 2013. URL : <http://cefr.revues.org/989>.
- Brun J.P., Munzi P., Botte E. (2017). Cuma. Il monumento funerario della "Sfinge" (A63) nella necropoli della Porta Mediana. *Complessi monumentali e arredo scultoreo nella Regio I Latium et Campania. Nuove scoperte e proposta di lettura in contesto*, Capaldi Gasparri, (eds), Atti del Convegno Internazionale, Napoli 5-6 Dicembre 2013. Quaderni del Centro studio Magna Grecia Vol. 24, Studi di antichità III, pp. 137-164.
- Castriota M., Cosco V., Barone T., De Santo G., Carafa P., Cazzanelli E. (2008). Micro-Raman characterizations of Pompei's mortars. *Journal of Raman Spectroscopy*, Vol. 39, pp. 295-301. doi:10.1002/jrs.1877.
- Cioni R., Santacroce R., Sbrana A. (1999). Pyroclastic deposits as a guide for reconstructing the multi-stage evolution of the Somma-Vesuvius Caldera. *Bulletin of Volcanology* Vol. 61, pp. 207-222. doi: 10.1007/s004450050272
- Colella A., Di Benedetto C., Calcaterra D., Cappelletti P., D'Amore M., Di Martire D., Graziano S.F., Papa L., de Gennaro M., Langella A. (2017). The Neapolitan Yellow Tuff: An outstanding example of heterogeneity. *Construction and Building Materials* Vol. 136, pp. 361-373. doi: 10.1016/j.conbuildmat.2017.01.053.
- Collepari M. (2003). La lezione dei romani: durabilità e sostenibilità delle opere architettoniche e strutturali. *Proceedings of III Convegno AIMAT "Restauro e Conservazione dei Beni Culturali: Materiali e Tecniche"*, Cassino, Italy.
- Covolani M., Lemaire B. (2017). Measuring the Roman building sites. The case of the opus reticulatum in the Necropolis of the Porta mediana in Cumae. *IMEKO International Conference on Metrology for Archaeology and Cultural Heritage* Lecce, Italy, October 23-25, 2017.
- De Bonis A., Febbraro S., Germinario C., Giampaola D., Grifa C., Guarino V., Langella A., Morra V. (2016). Distinctive Volcanic Material for the Production of Campana A Ware: The Workshop Area of Neapolis at the Duomo Metro Station in Naples, Italy. *Geoarchaeology* Vol. 31, pp 437-466. doi: 10.1002/geoa.21571.

- De Vita A., Pesaresi P., Puglisi V. (2010). Overview of the “100 Mortars Project” at the archaeological site of Herculaneum, Italy, in: *Proceedings of 2nd Historic Mortars Conference/HMC2010*, 22–24 September, 2010, Prague, 2010.
- Deino, A. L., Orsi G., de Vita S., Piochi M. (2004), The age of the Neapolitan Yellow Tuff caldera-forming eruption (Campi Flegrei caldera – Italy) assessed by  $^{40}\text{Ar}/^{39}\text{Ar}$  dating method, *Journal of Volcanology and Geothermal Research*, Vol. 133, pp. 157–70. doi: 10.1016/S0377-0273(03)00396-2.
- de’ Gennaro M., Cappelletti P., Langella A., Perrotta A., Scarpati C. (2000). Genesis of zeolites in the Neapolitan Yellow Tuff: geological, volcanological and mineralogical evidence. *Contributions to Mineralogy and Petrology* Vol. 139, pp. 17-35. doi: 10.1007/s004100050571.
- De Luca R., Miriello D., Pecci A., Dominguez-Bella S., Bernal-Casasola D., Cottica D., Bloise A., Crisci G.M. (2015). Archaeometric study of mortars from the garum shop at Pompeii, Campania, Italy, *Geoarchaeology* Vol. 30, pp. 330–351. doi: 10.1002/gea.21515.
- Drdacky M., Fratini F., Frankeova D., Slizkova Z. (2013). The Roman mortars used in the construction of the Ponte di Augusto (Narni, Italy). A comprehensive assessment. *Construction and building materials* Vol. 38, pp. 1117–1128. doi: 10.1016/j.conbuildmat.2012.09.044.
- Fedele L., Scarpati C., Lanphere M., Melluso L., Morra V., Perrotta A., Ricci G. (2008). The Breccia Museo formation, Campi Flegrei, southern Italy: geochronology, chemostratigraphy and relationship with the Campanian Ignimbrite eruption, *Bulletin of Volcanology*, Vol. 70, pp. 1189–219. doi: 10.1007/s00445-008-0197-y.
- Fedele, L., Insinga, D., Calvert, A. T., Morra, V., Perrotta, A., and Scarpati, C. (2011).  $^{40}\text{Ar}/^{39}\text{Ar}$  dating of tuff vents in the Campi Flegrei caldera (southern Italy): toward a new chronostratigraphic reconstruction of the Holocene volcanic activity, *Bulletin of Volcanology*, Vol. 73 (9), pp. 1323–36. doi: 10.1007/s00445-011-0478-8.
- Fernández R., Nebreda B., Vigil de la Villa R., García R., Frías M. (2010). Mineralogical and chemical evolution of hydrated phases in the pozzolanic reaction of calcined paper sludge. *Cement & Concrete Composites*, Vol. 32, pp. 775-782. doi: 10.1016/j.cemconcomp.2010.08.003.
- Gagliardi R., Kalin O., Morreale e., Palacca E., Scandone P., Sprugnoli R. (1980). Una banca dati geologici, CNR-PFG, 393. ESA, Roma.
- García R., Vigil de la Villa R., Rodríguez O., Frías M. (2009). Mineral phases formation on the pozzolana/lime/water system. *Applied Clay Science*, Vol. 43, pp. 331-335. doi: 10.1016/j.clay.2008.09.013.
- Guarino V., Wu F.Y., Melluso L., Gomes C.B., Tassinari C.C.G., Ruberti E., Brillì M. (2017). U-Pb ages, geochemistry, C-O-Nd-Sr-Hf isotopes and petrogenesis of the Catalão II carbonatitic complex (Alto Paranaíba Igneous Province, Brazil): implications for regional-scale heterogeneities in the Brazilian carbonatite associations. *International Journal of Earth Sciences* Vol. 106 (6) pp. 1963-1989. doi: 10.1007/s00531-016-1402-4.
- Izzo F., Arizzi A., Cappelletti P., Cultrone G., De Bonis A., Germinario C., Graziano S.F., Grifa C., Guarino V., Mercurio M., Morra, Langella A. (2016). The art of building in the Roman period (89 BC – 79 AD): Mortars plasters and mosaic floors from ancient Stabiae (Naples, Italy). *Construction and Building Materials*, Vol. 117, pp. 129–143. doi: 10.1016/j.conbuildmat.2016.04.101.
- Jackson M. D., Deocampo D., Marra F. and Scheetz B. (2010). Mid-Pleistocene Pozzolan volcanic Ash in Ancient Roman Concretes - *Geoarchaeology: An International Journal*, Vol. 25(1), pp. 36-74.
- Krumbein W.C. Sloss L.L. (1979). Stratigrafia e Sedimentazione, a cura di Ciocchini, Valletta C.E.R. Roma.
- Langella A., Bish D. L., Cappelletti P., Cerri G., Colella A., De Gennaro R., et al. (2013). New insights into the mineralogical facies distribution of Campanian Ignimbrite, a relevant Italian industrial material. *Applied Clay Science*, Vol. 72, pp. 55–73. doi: 10.1016/j.clay.2013.01.008.
- La Russa M.F., Ruffolo S.A, Ricca M., Rovella N., Comite V., Alvarez de Buergo M., Barca D., Crisci G.M. (2015). Archaeometric approach for the study of mortars from the underwater archaeological site of Baia (Naples) Italy: Preliminary results, *Periodico di Mineralogia* Vol 3, pp. 553–567. doi: 10.2451/2015PM0031.
- Le Maitre R. W., Bateman P., Dudek A., Keller J. (1989). A Classification of Igneous rocks and Glossary of Term: Recommendations of the International Union of Geological Sciences Subcommission on the Systematics of Igneous Rocks. *Blackwell Scientific Publications*, Oxford.
- Liritzis, I, Al-Otaibi, F, Kilikoglou, V, Perdikatsis, V, Polychroniadou, E, Drivaliari, A (2015) Mortar analysis of wall painting at Amfissa Cathedral for conservation-restoration purposes. *Mediterranean Archaeology and Archaeometry*, Vol. 15, No 3, pp. 301-311 (DOI: 10.5281/zenodo.33833)

- Melluso L., de' Gennaro R., Fedele, L., Franciosi, L., and Morra, V. (2012). Evidence of crystallization in residual, Cl-F-rich, agpaitic, trachyphonolitic magmas and primitive Mg-rich basalt-trachyphonolite interaction in the lava domes of the Phlegrean Fields (Italy), *Geological Magazine*, Vol. 149 (3), pp. 532-50. doi: 10.1017/S0016756811000902.
- Middendorf B., Hughes J.J., Callebaut K., Baronio G., Papayianni I. (2005). Investigative methods for the characterisation of historic mortars - Part 1: *Mineralogical characterization, Materials and Structures* Vol. 38, pp. 761-769. doi: 10.1007/BF02479289.
- Miriello D., Barca D., Bloise A., Ciarallo A., Crisci G.M., De Rose T., Gattuso C., Gazineo F., La Russa M.F. (2016). Characterisation of archaeological mortars from Pompeii (Campania, Italy) and identification of construction phases by compositional data analysis. *Journal of Archaeological Science* Vol. 37, pp 2207-2223. doi: 10.1016/j.jas.2010.03.019.
- Moropoulou A., Bakolas A., Bisbikou K., (2000). Characterization of ancient, byzantine and late historical mortars by thermal and x-ray diffraction techniques. *Termochimica Acta* 269/270, 819959a, pp 779-795.
- Morra V., Calcaterra D., Cappelletti P., Colella A., Fedele L., de' Gennaro R., Langella A., Mercurio M., de' Gennaro, M. (2010). Urban geology: relationships between geological setting and architectural heritage of the Neapolitan area, in *The geology of Italy: tectonics and life along plate margins* (eds. M. Beltrando, A. Peccerillo, M. Mattei, S. Conticelli and C. Doglioni), *Journal of the Virtual Explorer*, Vol. 36, paper 27. <http://virtualexplorer.com.au/journal/2010/36>.
- Orsi G., D'Antonio M., de Vita S., Gallo G. (1992). The Neapolitan Yellow Tuff, a large magnitude trachytic phreatoplinian eruption: eruptive dynamics, magma withdrawal and caldera collapse, *Journal of Volcanology and Geothermal Research*. Vol. 53, pp. 275- 287. doi: 10.1016/0377-0273(92)90086-S.
- Orsi G., de Vita S., Di Vito M. (1996). The restless, resurgent Campi Flegrei nested caldera (Italy): constraints on its evolution and configuration. *Journal of Volcanology and Geothermal Research*, Vol. 74, pp. 179-214. doi: 10.1016/S0377-0273(96)00063-7.
- Pappalardo L., Civetta L., D'Antonio M., Deino A., Di Vito M., Orsi G., Carandente A., De Vita S., Isaia R., Piochi M., (1999). Chemical and Sr-isotopic evolution of the Phlegrean magmatic system before the Campanian Ignimbrite and Neapolitan Yellow Tuff eruptions. *Journal of Volcanology and Geothermal Research*, Vol. 91, pp. 141-166. doi: 10.1016/S0377-0273(99)00033-5.
- Pecchioni E., Fratini F., Cantisani E. (2008). *Le malte antiche e moderne tra tradizione e innovazione*. Patròn (ed.), Bologna.
- Pecchioni E., Fratini F., Cantisani E. (2009). *Le malte. Testimonianza della cultura materiale nei siti archeologici*. *Restauro archeologico* Vol 2, pp. 25-27.
- Piovesan R., Dalconi M.C., Maritan L., Mazzoli C. (2013). X-rays powder diffraction clustering and quantitative phase analysis on historical mortars. *European Journal of Mineralogy* Vol. 25, pp. 165-175. doi: 10.1127/0935-1221/2013/0025-2263
- Ricci S., Davidde B., Bartolini M. and Priori G.F. (2009). Bioerosion of lapideous artefacts found in the archaeological site of Baia (Naples). *Archaeologia Marittima Mediterranea, An International Journal on Underwater Archaeology*, Vol. 6, pp. 167-186.
- Rispoli C., Esposito R., De Bonis A., Cappelletti P., Morra V., Talamo P. (2016). The Thermal Complex of Baia: preliminary characterization of mortars, in: *Un ponte tra arte e scienza: passato, presente e prospettive future*. Arcavacata di Rende (CS), 9-11 marzo 2016, AIAR - Associazione Italiana di Archeometria, 2016, p. 87.
- Rispoli C., Graziano S.F., De Bonis A., Cappelletti P., Esposito R., Talamo P. (2015). Piscina Mirabilis: characterization of geomaterials, in: *Proceedings of the 1st International Conference on Metrology for Archaeology*. Benevento, 22-23 ottobre 2015, 2015, pp. 266-270.
- Rolandi, G., Petrosino, P., Mc Greehin, J. (1998). The interplinian activity at Somma-Vesuvius in the last 3500 years. *Journal of Volcanology and Geothermal Research* Vol. 82, pp. 19-52.
- Rolandi, G., Bellocci, F., Cortini, M. (2004). A new model for the formation of the Somma Caldera. *Mineralogy and Petrology* Vol. 80, pp. 27-44.
- Salama, K.K, Ali, M.F, Moussa, A.M (2017) The presence of cement mortars in the added chambers of El Sakakeny Palace: a case study. *SCIENTIFIC CULTURE*, Vol. 3, No 3, pp. 25-29 (DOI: 10.5281/zenodo.813134)
- Siivola J., Rolf Schmid (2007). List of Mineral Abbreviations. *IUGS Recommendations*
- Vezzoli, L. (1988). Island of Ischia. C.N.R. *Quaderni de La ricerca scientifica* 114, Vol. 10, 134 pp.

- UNI-EN 11176 (2006). Beni culturali - Descrizione petrografica di una malta. Ed. UNI (Ente Nazionale Italiano Unificazione) Milano.
- UNI-EN 11305 (2009). Beni culturali - Malte storiche - *Linee guida per la caratterizzazione mineralogico-petrografica, fisica e chimica delle malte*. Ed. UNI (Ente Nazionale Italiano Unificazione) Milano.
- Vitruvius M.P., *De Architectura (On Architecture)*; 499 pp. *Harleian Manuscript 2767* and Translated into English, Vol. 2 Edited by F Granger (The Loeb classical Library). Heinemann, London, UK, 1962.
- Whitney D.L., Evans B.W. (2010). Abbreviations for names of rock-forming minerals. *American Mineralogist*, Vol. 95, pp. 185–187 doi: 10.2138/am.2010.3371.
- Yaseen I.A.B., Al-Amoush H., Al-Farajat M., Mayyas A. (2012). Petrography and mineralogy of Roman mortars from buildings of the ancient city of Jerash, Jordan. *Construction and Building Materials* Vol. 38, pp. 465–471. doi: 10.1016/j.conbuildmat.2012.08.022.